



Improved mass relations of mirror nuclei

Cheng Xu¹ · Man Bao¹

Received: 9 February 2024 / Revised: 23 April 2024 / Accepted: 27 April 2024 / Published online: 31 August 2024

© The Author(s), under exclusive licence to China Science Publishing & Media Ltd. (Science Press), Shanghai Institute of Applied Physics, the Chinese Academy of Sciences, Chinese Nuclear Society 2024

Abstract

In this study, we revisit the previous mass relations of mirror nuclei by considering $1/N$ - and $1/Z$ -dependent terms and the shell effect across a shell. The root-mean-squared deviation is 66 keV for 116 nuclei with neutron number $N \geq 10$, as compared with experimental data compiled in the AME2020 database. The predicted mass excesses of 173 proton-rich nuclei, including 98 unknown nuclei, are tabulated in the Supplemental Material herein with competitive accuracy.

Keywords Nuclear mass · Mirror nuclei · Proton-rich nuclei

1 Introduction

The nuclear mass $M(N, Z)$, where N and Z are the neutron and proton numbers of a nucleus, respectively, is a fundamental quantity for an atomic nucleus and is crucial in cosmology and astrophysics. Several theoretical methods exist for describing and predicting nuclear masses [1–3]. Examples include global models such as the Skyrme–Hartree–Fock–Bogoliubov theory [4–6], the finite-range droplet model [7–9], the Weizsäcker–Skyrme mass formula [10–13], and the relativistic continuum Hartree–Bogoliubov theory [14], as well as local models such as the Audi–Wapstra extrapolation method [15–19], the Garvey–Kelson mass relations [20–24] and their improvements [25–29], and mass relations based on neutron–proton interactions [30–33]. Furthermore, machine learning is widely used to study nuclear masses [34–38] and other physical quantities [39–42].

Additionally, researchers have developed some formulas based on isospin symmetry to predict the masses of mirror nuclei, such as the isobaric multiplet mass equation [43–46] and the improved Kelson–Garvey mass relations [47, 48]. Recently, a simple relationship correlating the Coulomb energy and shell effect was derived to describe the masses of

mirror nuclei with a root-mean-squared deviation (RMSD) of approximately 200 keV [49]. This relationship was further improved in other studies [50–54] and has expanded to unbound systems beyond the proton drip line [53].

The purpose of this study is to improve the mass relations of mirror nuclei presented in Ref. [53] by investigating the $1/N$ - and $1/Z$ -dependent terms and a simple shell correction. The improved relations are used to describe the experimental mass excesses of proton-rich nuclei with $N \geq 10$ with remarkable accuracy and to predict some unknowns. The remainder of this paper is organized as follows: In Sect. 2, we explain the improvements proposed using empirical formulas for one-nucleon separation energies. In Sect. 3, we investigate the predictive power of the improved mass relations for mirror nuclei. Finally, we conclude this paper in Sect. 4.

2 Improved mass relations of mirror nuclei

We begin our discussion with the mass relations of mirror nuclei presented in Ref. [53], which are defined as follows:

$$\begin{aligned} \Delta_n(N - k, Z) &\equiv [M(N - k - 1, Z) - M(N - k, Z)] \\ &\quad - [M(N, Z - k - 1) - M(N, Z - k)] \\ &= S_n(N - k, Z) - S_p(N, Z - k) - \Delta E_{np} \\ &= a_c \delta_c^n + (-)^{N-k} \beta (A - k)^{-1} - C, \end{aligned} \quad (1)$$

This work was supported by the National Natural Science Foundation of China (No. 11905130).

✉ Man Bao
mbao@usst.edu.cn

¹ Department of Physics, University of Shanghai for Science and Technology, Shanghai 200093, China

$$\begin{aligned} \Delta_p(N-k, Z) &\equiv [M(N-k, Z-1) - M(N-k, Z)] \\ &\quad - [M(N-1, Z-k) - M(N, Z-k)] \\ &= S_p(N-k, Z) - S_n(N, Z-k) + \Delta E_{np} \\ &= a_c \delta_c^p - (-)^Z \beta (A-k)^{-1} + C \end{aligned} \tag{2}$$

for $N = Z$, where k is an integer in the range of 1–4, S_n (S_p) is the one-neutron (one-proton) separation energy, $\Delta E_{np} \sim 0.782$ MeV represents the atomic mass difference between a neutron and proton, $A - k$ is the mass number ($A = N + Z$), and C is an adjustable constant. The terms with the parameter a_c correspond to sophisticated Coulomb energy terms [51], where

$$\begin{aligned} \delta_c^n &= (k+1)(A-k-2)(A-k-1)^{-1/3} \\ &\quad - k(A-k-1)(A-k)^{-1/3} - 0.808, \end{aligned} \tag{3}$$

$$\begin{aligned} \delta_c^p &= (k-1)(A-k-2)(A-k-1)^{-1/3} \\ &\quad - k(A-k-1)(A-k)^{-1/3} + 0.808, \end{aligned} \tag{4}$$

and β in Eqs. (1)–(2) is an optimized parameter that represents empirical odd-even staggering in the Coulomb energy [52].

Deviations between the theoretical and experimental values of Δ_n [Δ_p] calculated using Eq. (1) [Eq. (2)] based on the AME2020 database [19] are shown in Fig. 1 (a) [(b)]. The corresponding RMSDs and number of pairs of mirror nuclei considered (denoted by \mathcal{N}) are presented in the third and last columns of Table 1. Here, five experimental data with uncertainties greater than 100 keV are excluded in our calculations.

Fig. 1 (Color online) Panels (a) and (b) correspond to deviations between theoretical and experimental values of Δ_n and Δ_p calculated using Eqs. (1)–(2) [53], based on AME2020 database [19]. Red circles represent cases with $Z > 20$ and $N - k \leq 21$ (or 20) for $\Delta_n(N - k, Z)$ [or $\Delta_p(N - k, Z)$], and blue triangles represent cases with $Z > 28$ and $N - k \leq 29$ (or 28) for $\Delta_n(N - k, Z)$ [or $\Delta_p(N - k, Z)$]

Table 1 RMSDs (in keV) of Δ_n and Δ_p with $N - k \geq 10$ and $1 \leq k \leq 4$, based on AME2020 database [19]. Second column corresponds to improved mass relations of mirror nuclei presented by Eqs. (16)–(17), and third column corresponds to Eqs. (1)–(2) [53]. Last column \mathcal{N} denotes number of pairs of mirror nuclei considered. Last row (labeled by Δ) shows results obtained using unified parameters of Δ_n and Δ_p

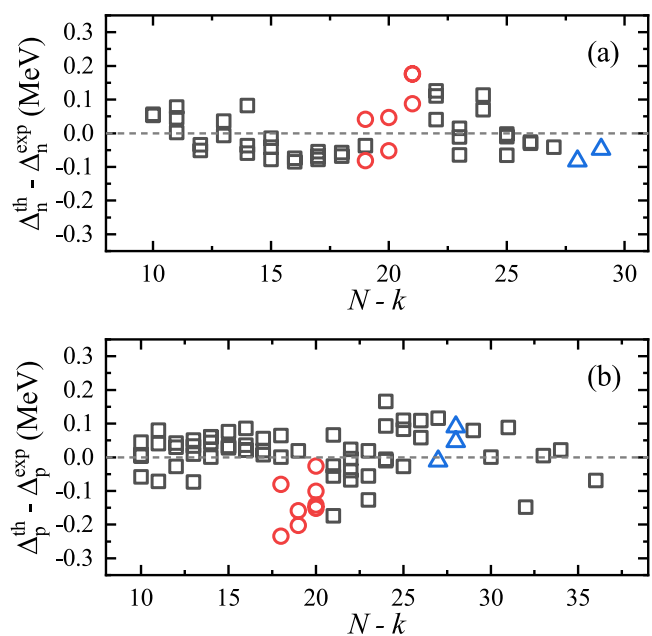
	This study	Eqs. (1)–(2)	\mathcal{N}
Δ_n	59	70	46
Δ_p	63	80	70
Δ	66	78	116

To improve the accuracies of Eqs. (1)–(2), we consider empirical formulas for the one-neutron separation energy S_n and one-proton separation energy S_p [55, 56], i.e.,

$$S_n = (a_1 + a_2 A^{1/3}) \frac{Z}{N} + a_3 + \delta_{\text{pair}} + \delta_{\text{sh}}, \tag{5}$$

$$S_p = (a_4 + a_5 A^{1/3}) \frac{N}{Z} + a_6 + \delta_{\text{pair}} + \delta_{\text{sh}} + \delta_{\text{coul}}, \tag{6}$$

where $\delta_{\text{coul}} = a_c Z A^{-1/3}$ is the Coulomb term; $\delta_{\text{pair}} = \pm a_p A^{-1/2}$ [the signs “+” and “−” correspond to S_n (S_p) of a nucleus with an even N (Z) and odd N (Z), respectively] is the pairing term; $\delta_{\text{sh}} = a_{\text{sh}} n$ is the empirical correction of the shell effect with n equaling 0, 1, 2, 3, and 4 for S_n (S_p) of a nucleus with N (Z) in the ranges of 1–28, 29–50, 51–82, 83–126, and above 127, respectively; and a_i are optimized parameters. The authors of [55] highlighted that Eqs. (5)–(6) show an N/Z dependence similar to the equations for S_n and S_p



derived from the approximate major-shell lowest-seniority mass equation [57], which is based on shell-structure calculations.

Based on Eqs. (1)–(2), Δ_n and Δ_p are related to the difference between S_n and S_p . Therefore, in reference to Eqs. (5)–(6), the terms dependent on Z/N and N/Z should remain, in addition to the Coulomb-energy and constant terms, which are well considered in Δ_n and Δ_p . Hence, the correction terms are written as

$$\begin{aligned} \delta_1^{\text{kn}} &= \frac{Z}{N-k}, \\ \delta_2^{\text{kn}} &= \frac{Z}{N-k}(A-k)^{1/3} \end{aligned} \tag{7}$$

for Δ_n , and

$$\begin{aligned} \delta_1^{\text{kp}} &= \frac{N-k}{Z}, \\ \delta_2^{\text{kp}} &= \frac{N-k}{Z}(A-k)^{1/3} \end{aligned} \tag{8}$$

for Δ_p , with $N = Z$. In Fig. 2 (a) [(c)], the experimental mass differences Δ_n (Δ_p) are plotted vs. δ_1^{kn} (δ_1^{kp}) based on the AME2020 database [19], where the black squares, red circles, blue triangles, and green stars correspond to the results of $k = 1, 2, 3$, and 4, respectively. Clearly, the growth rates of Δ_n and Δ_p differ depending on the value of k .

To avoid this difference in k , which results in excessive parameters, we consider the neutron–proton interaction between the last neutron and last proton (denoted by $\delta V_{\text{in-1p}}$) [32] of the two-mirror nuclei recommended in Ref. [50]. Here, $\delta V_{\text{in-1p}}$ is expressed as

$$\begin{aligned} \delta V_{\text{in-1p}}(N, Z) &= -M(N, Z) - M(N-1, Z-1) \\ &\quad + M(N-1, Z) + M(N, Z-1). \end{aligned} \tag{9}$$

Suppose that $\delta V_{\text{in-1p}}$ of the two-mirror nuclei are equal [50, 58]; therefore, we have $\delta V_{\text{in-1p}}(N-k, Z) \simeq \delta V_{\text{in-1p}}(N, Z-k)$. This equation can be rewritten as

$$\begin{aligned} &[M(N-k-1, Z) - M(N-k, Z)] \\ &- [M(N, Z-k-1) - M(N, Z-k)] \simeq \\ &[M(N-k-1, Z-1) - M(N-k, Z-1)] \\ &- [M(N-1, Z-k-1) - M(N-1, Z-k)] \end{aligned} \tag{10}$$

or

$$\begin{aligned} &[M(N-k, Z-1) - M(N-k, Z)] \\ &- [M(N-1, Z-k) - M(N, Z-k)] \simeq \\ &[M(N-k-1, Z-1) - M(N-k-1, Z)] \\ &- [M(N-1, Z-k-1) - M(N, Z-k-1)]. \end{aligned} \tag{11}$$

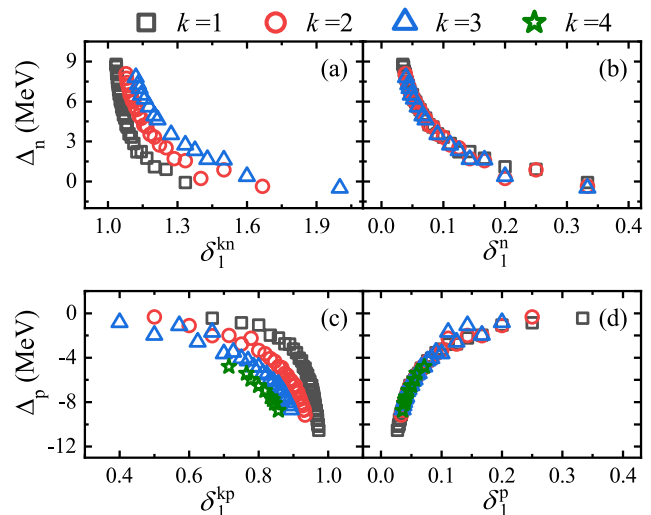


Fig. 2 (Color online) Panels (a) and (b) correspond to experimental mass differences Δ_n vs. δ_1^{kn} and δ_1^n ; and panels (c) and (d) correspond to experimental Δ_p vs. δ_1^{kp} and δ_1^p , respectively, based on AME2020 database [19]. Black squares, red circles, blue triangles, and green stars correspond to $k = 1, 2, 3$, and 4, respectively. Different growth rates of Δ_n and Δ_p shown in panels (a) and (c) are unified to a compact trajectory, as plotted in panels (b) and (d), respectively

Based on the definitions of Δ_n and Δ_p presented in Eqs. (1)–(2), Eqs. (10)–(11) are equivalent to

$$\begin{aligned} \Delta_n(N-k, Z) &\simeq \Delta_n(N-k, Z-1), \\ \Delta_p(N-k, Z) &\simeq \Delta_p(N-k-1, Z), \end{aligned} \tag{12}$$

which implies that Δ_n is approximately independent of Z for $N-k$, and Δ_p is approximately independent of $N-k$ for Z , when $k = 1-4$. Thus, the correction terms in Eqs. (7)–(8) can be rewritten as

$$\begin{aligned} \delta_1^n &= \frac{1}{N-k}, \\ \delta_2^n &= \frac{1}{N-k}(A-k)^{1/3} \end{aligned} \tag{13}$$

for Δ_n , and

$$\begin{aligned} \delta_1^p &= \frac{1}{Z}, \\ \delta_2^p &= \frac{1}{Z}(A-k)^{1/3} \end{aligned} \tag{14}$$

for Δ_p . Based on the AME2020 database [19], the experimental mass differences Δ_n (Δ_p) are plotted vs. δ_1^n (δ_1^p) in Fig. 2 (b) [(d)]. The growth rates of Δ_n and Δ_p are unified into a compact trajectory, as shown in panels (b) and (d), and are independent of k . This result is similar to the finding that strong linear correlations between Δ_n (Δ_p) and δ_c^n (δ_c^p) are independent of k , as mentioned in Ref. [50]. Thus, Δ_n (Δ_p) with different k can be calculated using unified parameters.

The other correction in this study pertains to the shell effect across a shell. Similar to the empirical correction of the shell effect for separation energies presented in Eqs. (5)–(6), we perform a simple correction for nuclei with neutron and proton numbers in different shells, i.e.,

$$\delta'_{sh} = \begin{cases} a_{sh1}, & Z > 20 \text{ and } N - k \leq 21 \text{ (or 20) for} \\ & \Delta_n(N - k, Z) \text{ [or } \Delta_p(N - k, Z)] \\ a_{sh2}, & Z > 28 \text{ and } N - k \leq 29 \text{ (or 28) for} \\ & \Delta_n(N - k, Z) \text{ [or } \Delta_p(N - k, Z)] \\ 0, & \text{others} \end{cases}, \quad (15)$$

where a_{sh1} and a_{sh2} are adjustable constants. Owing to the limitations of the experimental data, our calculation is restricted to nuclei with $Z < 50$. Thus, only the parameters for 20 and 28 shells are presented in Eq. (15).

Considering the two types of corrections discussed above [Eqs. (13)–(14) and Eq. (15)], our improved mass relations for mirror nuclei are written as follows:

$$\Delta_n(N - k, Z) = a_c \delta_c^n + (-)^{N-k} \beta (A - k)^{-1} + \alpha_1 \delta_1^n + \alpha_2 \delta_2^n + \delta'_{sh} - C, \quad (16)$$

$$\Delta_p(N - k, Z) = a_c \delta_c^p - (-)^Z \beta (A - k)^{-1} - \alpha_1 \delta_1^p - \alpha_2 \delta_2^p - \delta'_{sh} + C, \quad (17)$$

for $N = Z$, where a_i , α_i , β , and C are optimized parameters; δ_c^n and δ_c^p are presented in Eq. (3) and Eq. (4), respectively.

Based on the AME2020 database [19], the RMSDs of our improved $\Delta_n(N - k, Z)$ and $\Delta_p(N - k, Z)$ [Eqs. (16)–(17)] with $N - k \geq 10$ are presented in the second column of Table 1. To reduce the total number of parameters, we assume the same parameters for Δ_n and Δ_p , and the results are presented in the last row of Table 1, labeled by Δ . Unification reduced the total number of parameters from 14 to 7, with a slight change in the RMSD. The results obtained using Eqs. (1)–(2) [53] are provided for comparison. As shown, our improvements were highly efficient, with the RMSD decreasing from 78 to 66 keV for 116 pairs of mirror nuclei.

Table 2 presents the optimized parameters of Δ obtained via least-squares fitting. As shown, the value of parameter a_c is reasonably close to its typical value of 0.70–0.72 MeV, whereas the value of parameter C is much smaller than the expected value of 0.782 MeV because its contribution is

included partly in our correction terms. Notably, the signs of parameters a_{sh1} and a_{sh2} are opposite. This is consistent with the results presented in Fig. 1, where the red circles (representing cases of a_{sh1}) are almost above (below) the dashed gray line for Δ_n (Δ_p), and the blue triangles (representing cases of a_{sh2}) indicate the opposite.

3 Prediction of masses for proton-rich nuclei

Our improved mass relations for mirror nuclei allow one to predict unknown masses of proton-rich nuclei with $10 < Z < 50$. Based on Eqs. (1)–(2), we obtain

$$M^{th}(N - k - 1, Z) = M(N - k, Z) + M(N, Z - k - 1) - M(N, Z - k) + \Delta_n^{th}(N - k, Z), \quad (18)$$

$$M^{th}(N - k, Z) = M(N - k, Z - 1) + M(N, Z - k) - M(N - 1, Z - k) - \Delta_p^{th}(N - k, Z), \quad (19)$$

with $1 \leq k \leq 4$, where $\Delta_n^{th}(N - k, Z)$ and $\Delta_p^{th}(N - k, Z)$ are calculated using Eqs. (16)–(17) with the unified parameters.

Based on Eqs. (18)–(19), up to two masses (M_i^{th}) can be predicted for a nucleus, and their average value with the weight of the theoretical uncertainties (σ_i) is considered as the predicted mass M^{th} , i.e.,

$$M^{th} = F \frac{M_1^{th}}{(\sigma_1)^2} + F \frac{M_2^{th}}{(\sigma_2)^2}, \quad (20)$$

$$F = \left[\frac{1}{(\sigma_1)^2} + \frac{1}{(\sigma_2)^2} \right]^{-1}.$$

The theoretical uncertainty of M^{th} is defined as $\sigma = \sqrt{F}$ [50]. Here, $(\sigma_i)^2$ ($i = 1, 2$) is the squared RMSD of Δ plus the sum of squared experimental uncertainties of the masses of the nuclei involved in the calculation.

To investigate the predictive powers of Eqs. (18)–(20), we predicted the masses of proton-rich nuclei based on the AME1995 [15], AME2003 [16], AME2012 [17], and AME2016 [18] databases, and then compared the predictions with experimental values obtained from the AME2020 database [19]. The RMSDs (denoted by σ_{95} , σ_{03} , σ_{12} , and σ_{16} , respectively) and the corresponding number of predictions

Table 2 Unified parameters (in keV) of improved $\Delta_n(N - k, Z)$ and $\Delta_p(N - k, Z)$ [Eqs. (16)–(17)] for nuclei with $N - k \geq 10$ and $1 \leq k \leq 4$, based on AME2020 database [19]

a_c	β	α_1	α_2	a_{sh1}	a_{sh2}	C
678	2198	537	−1761	−122	43	317

considered (denoted by \mathcal{N}_{pre}) are presented in the third and last columns of Table 3, respectively. The results in (out) parentheses correspond to cases that include (exclude) experimental data with uncertainties greater than 100 keV. The RMSDs of Ref. [53] are listed in the second column for comparison, which indicate the competitiveness of our predictions. Based on the AME2020 database [19], the mass excesses of 173 proton-rich nuclei (including 98 unknowns) with $10 < Z < 50$ were predicted and are tabulated in the Supplementary Material [59] along with the corresponding theoretical uncertainties.

In Fig. 3, the predicted masses of eight nuclei are presented (labeled with red circles) with respect to those presented in the AME2020 database [19]. Panels (a)–(e) correspond to five nuclei with experimental uncertainties greater than 100 keV [19], whose experimental masses are excluded from our calculations, as mentioned in Sect. 2; panel (f) corresponds to the nucleus, in which the unbound nature is confirmed experimentally [60, 61]; and panels (g) and (h)

Table 3 RMSDs (in keV) of predicted masses of proton-rich nuclei compared with experimental data obtained from AME2020 database [19]. σ_{95} , σ_{03} , σ_{12} , and σ_{16} correspond to extrapolation based on AME1995 [15], AME2003 [16], AME2012 [17], and AME2016 [18] databases, respectively. Last column \mathcal{N}_{pre} denotes number of predictions considered. Results in (out) parentheses correspond to cases including (excluding) experimental data with uncertainties greater than 100 keV. Results of Ref. [53] are listed in second column for comparison

	Ref. [53]	This study	\mathcal{N}_{pre}
σ_{95}	113 (146)	90 (133)	19 (25)
σ_{03}	116 (210)	95 (198)	20 (20)
σ_{12}	76 (72)	77 (68)	11 (9)
σ_{16}	84 (79)	84 (74)	8 (7)

correspond to nuclei with recent new measurements (labeled by green diamonds) [62]. The predicted masses obtained from Ref. [53] (labeled with blue triangles) are provided for comparison. Our predicted masses are more similar to the experimental values and show significantly lower theoretical uncertainties, except for ^{55}Cu in panel (c).

For ^{61}Ga in Fig. 3 (g), the recent experimental mass is -47114 (12) keV [62], which is three times more precise than the experimental value provided in the AME2020 database [19], i.e., -47134.7 (38.0) keV. The mass of ^{60}Ga , as shown in Fig. 3, (h) was recently measured to be -40005 (30) keV [62], which is more than 400 keV less than the estimated value presented in AME2020 [19], i.e., $-39590^{#}(200^{#})$ keV. Our predictions for the masses of both nuclei are more similar to their new measurements, in comparison with the values presented in Ref. [53].

Table 4 lists the predicted masses and those presented in Ref. [52], Ref. [53], and Ref. [54] for comparison with the newly measured experimental values obtained from Ref. [63]. The corresponding RMSDs are listed in the last two rows of Table 4, where σ'_1 and σ'_2 denote the RMSDs for all the 12 nuclei and the same six nuclei in Ref. [52], respectively. Our predictions agree well with the experimental values, and the RMSD can be further reduced to 48 keV for nine nuclei, excluding ^{65}As , ^{70}Kr , and ^{75}Sr , whose experimental uncertainties are greater than 100 keV.

4 Summary

In this study, we revisited the mass relations of mirror nuclei proposed in Ref. [49] and improved in Ref. [53] by considering $1/N$ - and $1/Z$ -dependent terms and the shell effect across a shell, which originated from the empirical formulas of

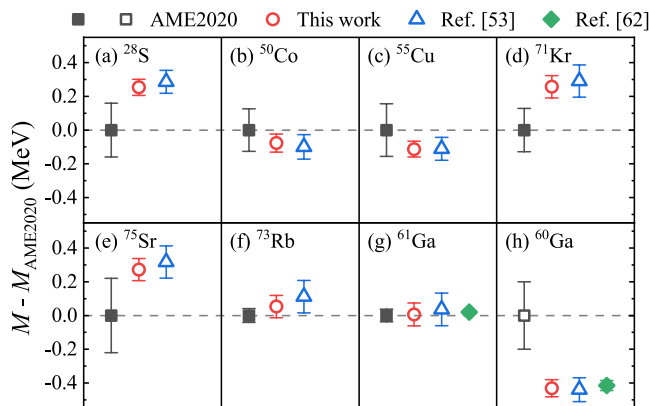


Fig. 3 (Color online) Nuclear masses deviating from those in AME2020 database [19]. Solid (hollow) black squares correspond to experimental (estimated) values obtained from AME2020 database [19]. Masses predicted in this study and Ref. [53] are labelled by hol-

low red circles and blue triangles, respectively, and recent measurements obtained from Ref. [62] are labeled by solid green diamonds. Experimental and theoretical uncertainties are labeled as well

Table 4 Newly measured nuclei masses (in keV) obtained from Ref. [63] and their predictions obtained from Ref. [52], Ref. [53], Ref. [54], and our improved relations [Eqs. (18)–(20)]. Values in parentheses indicate corresponding experimental or theoretical uncertainties. σ'_1 and σ'_2 (in keV) in last two rows correspond to RMSDs between theoretical and measured values [63] for all 12 nuclei and the same six nuclei presented in Ref. [52], respectively

Nuclei	Ref. [63]	Ref. [52]	Ref. [53]	Ref. [54]	This work
^{58}Zn	−42248(36)	−42319(82)	−42334(68)	−42327(41)	−42327(47)
^{60}Ga	−40034(46)	−39995(84)	−40030(71)	−39982(41)	−40022(50)
^{61}Ga	−47168(21)	–	−47099(97)	−47085(44)	−47129(68)
^{62}Ge	−42289(37)	−42332(86)	−42328(73)	−42349(41)	−42373(54)
^{63}Ge	−46978(15)	–	−47010(96)	−46993(41)	−47022(66)
^{64}As	−39710(110)	−39662(93)	−39512(82)	−39562(41)	−39601(62)
^{65}As	−46806(42)	–	−46751(96)	−46760(41)	−46790(66)
^{66}Se	−41982(61)	−42046(98)	−41847(88)	−41890(41)	−41985(71)
^{67}Se	−46549(20)	–	−46581(96)	−46588(41)	−46604(66)
^{70}Kr	−41320(140)	−41560(101)	−41269(96)	−41333(41)	−41320(78)
^{71}Kr	−46056(24)	–	−46037(96)	−46068(42)	−46070(66)
^{75}Sr	−46200(150)	–	−46302(96)	−46356(41)	−46346(66)
σ'_1	–	–	86	81	67
σ'_2	–	110	107	85	65

one-nucleon separation energies. The improvements of our formulas were shown to be effective for nuclei with neutron number $N \geq 10$, as indicated by an RMSD of only 66 keV for 116 pairs of mirror nuclei, as compared with the experimental data presented in the AME2020 database [19] and 90 keV for 19 proton-rich nuclei extrapolated from databases AME1995 [15] to AME2020 [19] (excluding experimental data with uncertainties greater than 100 keV).

The predicted mass excesses of proton-rich nuclei with $10 < Z < 50$, based on the AME2020 database [19] and our improved formulas, as well as the corresponding theoretical uncertainties, were tabulated, as presented in the Supplementary Material [59]. These predictions agreed well with the newly measured nuclei masses [63], with an RMSD of only 67 keV for 12 nuclei. The RMSD was further reduced to 48 keV by excluding three experimental data, with uncertainties greater than 100 keV. We believe that these predictions of proton-rich nuclei provide valuable information for investigations pertaining to nuclear physics, such as two-proton radioactivity [64].

Author Contributions All authors contributed to the study conception and design. Material preparation, data collection and analysis were performed by Cheng Xu and Man Bao. The first draft of the manuscript was written by Cheng Xu and all authors commented on previous versions of the manuscript. All authors read and approved the final manuscript.

Data Availability Statement The data that support the findings of this study are openly available in Science Data Bank at <https://cstr.cn/31253.11.sciencedb.j00186.00149> and <https://doi.org/10.57760/sciencedb.j00186.00149>.

Declarations

Conflict of interest The authors declare that they have no Conflict of interest.

References

1. D. Lunney, J.M. Pearson, C. Thibault, Recent trends in the determination of nuclear masses. *Rev. Mod. Phys.* **75**, 1021 (2003). <https://doi.org/10.1103/RevModPhys.75.1021>
2. M. Bao, H. Jiang, Y.M. Zhao, Systematic study on nuclear mass and related physical quantities. *Nucl. Phys. Rev.* **40**, 141 (2023). <https://doi.org/10.11804/NuclPhysRev.40.2022098>
3. M. Bao, H. Jiang, Y.M. Zhao, Atomic mass excesses and related physical quantities & nuclear charge radii. V2. *Science Data Bank* (2023). <https://doi.org/10.57760/sciencedb.j00177.00003>
4. S. Goriely, M. Samyn, M. Bender et al., Further explorations of Skyrme-Hartree-Fock-Bogoliubov mass formulas. II. Role of the effective mass. *Phys. Rev. C* **68**, 054325 (2003). <https://doi.org/10.1103/PhysRevC.68.054325>
5. S. Goriely, N. Chamel, J.M. Pearson, Skyrme-Hartree-Fock-Bogoliubov nuclear mass formulas: crossing the 0.6 MeV accuracy threshold with microscopically deduced pairing. *Phys. Rev. Lett.* **102**, 152503 (2009). <https://doi.org/10.1103/PhysRevLett.102.152503>
6. S. Goriely, N. Chamel, J.M. Pearson, Further explorations of Skyrme-Hartree-Fock-Bogoliubov mass formulas. XVI. Inclusion of self-energy effects in pairing. *Phys. Rev. C* **93**, 034337 (2016). <https://doi.org/10.1103/PhysRevC.93.034337>
7. P. Möller, W.D. Myers, W.J. Swiatecki et al., Nuclear mass formula with a finite-range droplet model and a folded-Yukawa single-particle potential. *At. Data Nucl. Data Tables* **39**, 225 (1988). [https://doi.org/10.1016/0092-640X\(88\)90023-X](https://doi.org/10.1016/0092-640X(88)90023-X)
8. P. Möller, J.R. Nix, W.D. Myers et al., Nuclear Ground-State Masses and Deformations. *At. Data Nucl. Data Tables* **59**, 185 (1995). <https://doi.org/10.1006/adnd.1995.1002>
9. P. Möller, A. Sierk, T. Ichikawa et al., Nuclear ground-state masses and deformations: FRDM(2012). *At. Data Nucl. Data Tables* **109–110**, 1 (2016). <https://doi.org/10.1016/j.adt.2015.10.002>
10. N. Wang, M. Liu, X. Wu, Modification of nuclear mass formula by considering isospin effects. *Phys. Rev. C* **81**, 044322 (2010). <https://doi.org/10.1103/PhysRevC.81.044322>
11. N. Wang, Z. Liang, Min Liu et al., Mirror nuclei constraint in nuclear mass formula. *Phys. Rev. C* **82**, 044304 (2010). <https://doi.org/10.1103/PhysRevC.82.044304>

12. M. Liu, N. Wang, Y. Deng et al., Further improvements on a global nuclear mass model. *Phys. Rev. C* **84**, 014333 (2011). <https://doi.org/10.1103/PhysRevC.84.014333>
13. N. Wang, M. Liu, X. Wu et al., Surface diffuseness correction in global mass formula. *Phys. Lett. B* **734**, 215 (2014). <https://doi.org/10.1016/j.physletb.2014.05.049>
14. X.W. Xia, Y. Lim, P.W. Zhao et al., The limits of the nuclear landscape explored by the relativistic continuum Hartree-Bogoliubov theory. *At. Data Nucl. Data Tables* **121–122**, 1 (2018). <https://doi.org/10.1016/j.adt.2017.09.001>
15. G. Audi, A.H. Wapstra, The 1995 update to the atomic mass evaluation. *Nucl. Phys. A* **595**, 409 (1995). [https://doi.org/10.1016/0375-9474\(95\)00445-9](https://doi.org/10.1016/0375-9474(95)00445-9)
16. G. Audi, A.H. Wapstra, C. Thibault, The Ame2003 atomic mass evaluation: (II). Tables, graphs and references. *Nucl. Phys. A* **729**, 337 (2003). <https://doi.org/10.1016/j.nuclphysa.2003.11.003>
17. M. Wang, G. Audi, A.H. Wapstra et al., The AME2012 atomic mass evaluation (II). Tables, graphs and references. *C* **36**, 1603 (2012). <https://doi.org/10.1088/1674-1137/36/12/003>
18. M. Wang, G. Audi, F.G. Kondev et al., The AME2016 atomic mass evaluation (II). Tables, graphs and references. *C* **41**, 030003 (2017). <https://doi.org/10.1088/1674-1137/41/3/030003>
19. M. Wang, W.J. Huang, F.G. Kondev et al., The AME 2020 atomic mass evaluation (II). Tables, graphs and references. *Chin. Phys. C* **45**, 030003 (2021). <https://doi.org/10.1088/1674-1137/abddaf>
20. G.T. Garvey, I. Kelson, New nuclidic mass relationship. *Phys. Rev. Lett.* **16**, 197 (1966). <https://doi.org/10.1103/PhysRevLett.16.197>
21. G.T. Garvey, W.J. Gerace, R.L. Jaffe et al., Set of nuclear-mass relations and a resultant mass table. *Rev. Mod. Phys.* **41**, S1 (1969). <https://doi.org/10.1103/RevModPhys.41.S1>
22. Z.C. Gao, Y.S. Chen, J. Meng, Garvey-Kelson mass relations and n-p interaction. *Chin. Phys. Lett.* **18**, 1186 (2001). <https://doi.org/10.3321/j.issn:0256-307X.2001.09.010>
23. Z. He, M. Bao, Y.M. Zhao et al., New features of the Garvey-Kelson mass relations. *Phys. Rev. C* **87**, 057304 (2013). <https://doi.org/10.1103/PhysRevC.87.057304>
24. Y.Y. Cheng, Y.M. Zhao, A. Arima, Strong correlations of the Garvey-Kelson mass relations. *Phys. Rev. C* **89**, 061304(R) (2014). <https://doi.org/10.1103/PhysRevC.89.061304>
25. J. Barea, A. Frank, J.G. Hirsch et al., Garvey-Kelson relations and the new nuclear mass tables. *Phys. Rev. C* **77**, 041304(R) (2008). <https://doi.org/10.1103/PhysRevC.77.041304>
26. I.O. Morales, A. Frank, Improving nuclear mass predictions through the Garvey-Kelson relations. *Phys. Rev. C* **83**, 054309 (2011). <https://doi.org/10.1103/PhysRevC.83.054309>
27. M. Bao, Z. He, Y. Lu et al., Generalized Garvey-Kelson mass relations. *Phys. Rev. C* **88**, 064325 (2013). <https://doi.org/10.1103/PhysRevC.88.064325>
28. M. Bao, Z. He, Y.Y. Cheng et al., Optimal channels of the Garvey-Kelson mass relations in extrapolation. *Sci. China Phys. Mech. Astron.* **60**, 022011 (2017). <https://doi.org/10.1007/s11433-016-0406-1>
29. Y.Y. Cheng, H. Jiang, Y.M. Zhao et al., Improved mass extrapolations by the Garvey-Kelson relations. *J. Phys. G Nucl. Part. Phys.* **44**, 115102 (2017). <https://doi.org/10.1088/1361-6471/aa8a25>
30. G.J. Fu, H. Jiang, Y.M. Zhao et al., Nuclear binding energies and empirical proton-neutron interactions. *Phys. Rev. C* **82**, 034304 (2010). <https://doi.org/10.1103/PhysRevC.82.034304>
31. H. Jiang, G.J. Fu, Y.M. Zhao et al., Nuclear mass relations based on systematics of proton-neutron interactions. *Phys. Rev. C* **82**, 054317 (2010). <https://doi.org/10.1103/PhysRevC.82.054317>
32. G.J. Fu, Y. Lei, H. Jiang et al., Description and evaluation of nuclear masses based on residual proton-neutron interactions. *Phys. Rev. C* **84**, 034311 (2011). <https://doi.org/10.1103/PhysRevC.84.034311>
33. H. Jiang, G.J. Fu, B. Sun et al., Predictions of unknown masses and their applications. *Phys. Rev. C* **85**, 054303 (2012). <https://doi.org/10.1103/PhysRevC.85.054303>
34. H.F. Zhang, L.H. Wang, J.P. Yin et al., Performance of the Levenberg-Marquardt neural network approach in nuclear mass prediction. *J. Phys. G Nucl. Part. Phys.* **44**, 045110 (2017). <https://doi.org/10.1088/1361-6471/aa5d78>
35. Z.M. Niu, J.Y. Fang, Y.F. Niu, Comparative study of radial basis function and Bayesian neural network approaches in nuclear mass predictions. *Phys. Rev. C* **100**, 054311 (2019). <https://doi.org/10.1103/PhysRevC.100.054311>
36. Y.F. Liu, C. Su, J. Liu et al., Improved naive Bayesian probability classifier in predictions of nuclear mass. *Phys. Rev. C* **104**, 014315 (2021). <https://doi.org/10.1103/PhysRevC.104.014315>
37. Z.P. Gao, Y.J. Wang, H.L. Lü et al., Machine learning the nuclear mass. *Nucl. Sci. Tech.* **32**, 109 (2021). <https://doi.org/10.1007/s41365-021-00956-1>
38. X.C. Ming, H.F. Zhang, R.R. Xu et al., Nuclear mass based on the multi-task learning neural network method. *Nucl. Sci. Tech.* **33**, 48 (2022). <https://doi.org/10.1007/s41365-022-01031-z>
39. X.B. Wei, H.L. Wei, Y.T. Wang et al., Multiple-models predictions for drip line nuclides in projectile fragmentation of $^{40,48}\text{Ca}$, $^{58,64}\text{Ni}$, and $^{78,86}\text{Kr}$ at 140 MeV/u. *Nucl. Sci. Tech.* **33**, 155 (2022). <https://doi.org/10.1007/s41365-022-01137-4>
40. B.S. Cai, C.X. Yuan, Random forest-based prediction of decay modes and half-lives of superheavy nuclei. *Nucl. Sci. Tech.* **34**, 204 (2023). <https://doi.org/10.1007/s41365-023-01354-5>
41. W. He, Q. Li, Y. Ma et al., Machine learning in nuclear physics at low and intermediate energies. *Sci. China Phys. Mech. Astron.* **66**, 282001 (2023). <https://doi.org/10.1007/s11433-023-2116-0>
42. Z. Gao, Q. Li, Studies on several problems in nuclear physics by using machine learning. *Nucl. Tech.* **46**, 95–102 (2023). <https://doi.org/10.11889/j.0253-3219.2023.hjs.46.080009>
43. S. Weinberg, S.B. Treiman, Electromagnetic Corrections to Isotopic Spin Conservation. *Phys. Rev.* **116**, 465 (1959). <https://doi.org/10.1103/PhysRev.116.465>
44. G.T. Garvey, Nuclear Mass Relations. *Annu. Rev. Nucl. Sci.* **19**, 433 (1969). <https://doi.org/10.1146/annurev.ns.19.120169.002245>
45. W. Benenson, E. Kashy, Isobaric quartets in nuclei. *Rev. Mod. Phys.* **51**, 527 (1979). <https://doi.org/10.1103/RevModPhys.51.527>
46. J. Britz, A. Pape, M.S. Antony, Coefficients of the isobaric mass equation and their correlations with various nuclear parameters. *At. Data Nucl. Data Tables* **69**, 125 (1998). <https://doi.org/10.1006/adnd.1998.0773>
47. I. Kelson, G.T. Garvey, Masses of nuclei with $Z > N$. *Phys. Lett.* **23**, 689 (1966). [https://doi.org/10.1016/0031-9163\(66\)91102-4](https://doi.org/10.1016/0031-9163(66)91102-4)
48. J. Tian, N. Wang, C. Li et al., Improved Kelson-Garvey mass relations for proton-rich nuclei. *Phys. Rev. C* **87**, 014313 (2013). <https://doi.org/10.1103/PhysRevC.87.014313>
49. M. Bao, Y. Lu, Y.M. Zhao et al., Simple relations between masses of mirror nuclei. *Phys. Rev. C* **94**, 044323 (2016). <https://doi.org/10.1103/PhysRevC.94.044323>
50. Y.Y. Zong, M.Q. Lin, M. Bao et al., Mass relations of corresponding mirror nuclei. *Phys. Rev. C* **100**, 054315 (2019). <https://doi.org/10.1103/PhysRevC.100.054315>
51. Y.Y. Zong, C. Ma, Y.M. Zhao et al., Mass relations of mirror nuclei. *Phys. Rev. C* **102**, 024302 (2020). <https://doi.org/10.1103/PhysRevC.102.024302>
52. C. Ma, Y.Y. Zong, Y.M. Zhao et al., Mass relations of mirror nuclei with local correlations. *Phys. Rev. C* **102**, 024330 (2020). <https://doi.org/10.1103/PhysRevC.102.024330>
53. Y.Y. Zong, C. Ma, M.Q. Lin et al., Mass relations of mirror nuclei for both bound and unbound systems. *Phys. Rev. C* **105**, 034321 (2022). <https://doi.org/10.1103/PhysRevC.105.034321>

54. S.T. Guo, Y.X. Yu, Z. Wang et al., Atomic mass relations of mirror nuclei. *Phys. Rev. C* **109**, 014304 (2024). <https://doi.org/10.1103/PhysRevC.109.014304>
55. K. Vogt, T. Hartmann, A. Zilges, Simple parametrization of single- and two-nucleon separation energies in terms of the neutron to proton ratio N/Z . *Phys. Lett. B* **517**, 255 (2001). [https://doi.org/10.1016/S0370-2693\(01\)01014-0](https://doi.org/10.1016/S0370-2693(01)01014-0)
56. M. Bao, Z. He, Y.M. Zhao et al., Empirical formulas for nucleon separation energies. *Phys. Rev. C* **87**, 044313 (2013). <https://doi.org/10.1103/PhysRevC.87.044313>
57. N. Zeldes, Nuclear energies and the shell model. *Nucl. Phys.* **7**, 27 (1958). [https://doi.org/10.1016/0029-5582\(58\)90238-4](https://doi.org/10.1016/0029-5582(58)90238-4)
58. J. Jänecke, Neutron-Proton Interaction in Mirror Nuclei. *Phys. Rev. C* **6**, 467 (1972). <https://doi.org/10.1103/PhysRevC.6.467>
59. C. Xu, M. Bao, Mass excesses of proton-rich nuclei with $10 < Z < 50$. calculated based on the AME2020 database and present formulas. V1. Science Data Bank, (2024). <https://doi.org/10.57760/sciencedb.j00186.00149>
60. H. Suzuki, L. Sinclair, P.A. Söderström et al., Discovery of ^{72}Rb : A Nuclear Sandbank Beyond the Proton Drip Line. *Phys. Rev. Lett.* **119**, 192503 (2017). <https://doi.org/10.1103/PhysRevLett.119.192503>
61. D.E.M. Hoff, A.M. Rogers, Z. Meisel et al., Influence of ^{73}Rb on the ashes of accreting neutron stars. *Phys. Rev. C* **102**, 045810 (2020). <https://doi.org/10.1103/PhysRevC.102.045810>
62. S.F. Paul, J. Bergmann, J.D. Cardona et al., Mass measurements of $^{60-63}\text{Ga}$ reduce x-ray burst model uncertainties and extend the evaluated $T = 1$ isobaric multiplet mass equation. *Phys. Rev. C* **104**, 065803 (2021). <https://doi.org/10.1103/PhysRevC.104.065803>
63. M. Wang, Y.H. Zhang, X. Zhou et al., Mass measurements of Upper fp -Shell $N = Z - 2$ and $N = Z - 1$ Nuclei and the Importance of Three-Nucleon Force along the $N = Z$ Line. *Phys. Rev. Lett.* **130**, 192501 (2023). <https://doi.org/10.1103/PhysRevLett.130.192501>
64. L. Zhou, S.M. Wang, D.Q. Fang et al., Recent progress in two-proton radioactivity. *Nucl. Sci. Tech.* **33**, 105 (2022). <https://doi.org/10.1007/s41365-022-01091-1>

Springer Nature or its licensor (e.g. a society or other partner) holds exclusive rights to this article under a publishing agreement with the author(s) or other rightsholder(s); author self-archiving of the accepted manuscript version of this article is solely governed by the terms of such publishing agreement and applicable law.